MULTIMODAL PASSIVE VIBRATION CONTROL OF SANDWICH BEAMS WITH SHUNTED SHEAR PIEZOELECTRIC MATERIALS

Marcelo A. Trindade, trindade@sc.usp.br
Carlos Eduardo B. Maio, carlosbmaio@yahoo.com.br
Mechanical Engineering Department, São Carlos School of Engineering, University of São Paulo, São Carlos, SP, Brazil

Abstract. *This work presents a performance analysis of multimodal passive vibration control of a sandwich beam using shear piezoelectric materials, embedded in a sandwich beam core, connected to independent resistive shunt circuits. Shear piezoelectric actuators were recently shown to be more interesting for higher frequencies and stiffer structures. In particular for shunted damping, it was shown that equivalent material loss factors of up to 31% can be achieved by optimizing the shunt circuit. In the present work, special attention is given to the design of multimodal vibration control through independent shunted shear piezoelectric sensors. In particular, a parametric analysis is performed to evaluate optimal configurations for a set of modes to be damped. Then, a methodology to evaluate the modal damping resulting from each shunted piezoelectric sensor is presented using the Modal Strain Energy method. Results show that modal damping factors of more than 1% can be obtained for three selected vibration modes.*

Keywords*: Vibration control, piezoelectric materials, shear piezoelectric sensors, shunt circuits, sandwich beams.*

1. INTRODUCTION

The use of piezoelectric materials for the vibration control of flexible structures has been widely studied in the last two decades. These materials seem to be well adapted to distributed control of structural vibrations since they are produced as very thin patches and layers that can be embedded in a laminate or composite structure and allow direct connection with an input/output electrical signal (Sunar and Rao, 1999). Although most of the studies present surface-bonded extension piezoelectric patches, acting as actuators and sensors, it is also possible to embed thickness-shear mode piezoelectric patches in replacement of an internal layer of a laminate structure, or part of it. This is obtained through longitudinally-poled piezoelectric patches that, when subjected to through-thickness electric fields, present shear strains (Sun and Zhang, 1995). It has been shown that piezoelectric actuators using their thickness-shear mode can be more effective than surface-mounted extension piezoelectric actuators for vibration damping (Trindade, Benjeddou and Ohayon, 1999; Raja, Prathap and Sinha, 2002; Baillargeon and Vel, 2005).

However, their use in connection to shunt circuits to provide passive vibration control is much less explored. The idea of connecting piezoelectric patches to shunt circuits is basically to control the mechanical energy via the electrical energy induced in the shunt circuit due to electromechanical coupling in the piezoelectric (Forward, 1979; Hagood and von Flotow, 1991). Most of the recent studies focus on optimizing the shunt circuits by including resistances, inductances and capacitances in series and/or parallel. Nevertheless, few studies focus on the optimization of the electromechanical coupling in the piezoelectric material. In particular, it was shown that the use of piezoelectric patches in thickness-shear mode may be more interesting since the electromechanical coupling is higher than that in extension mode (Benjeddou and Ranger-Vieillard, 2004; Benjeddou, 2006; Trindade and Maio, 2006). Therefore, the present work reports recent studies on the use of thickness-shear piezoelectric patches connected to resistive shunt circuits for the passive vibration control of sandwich beams.

2. THEORETICAL FORMULATION

This section presents a theoretical model for the electromechanical response of a shear piezoelectric patch connected to a shunt circuit. The methodology adopted here is the impedance-based formulation put forward by Hagood and von Flotow (1991) and recently applied to shear piezoelectric actuators by Benjeddou and Ranger-Vieillard (2004).

2.1. Shunted Shear Piezoelectric Model

For a one-dimensional shear stress loading of a longitudinally poled piezoelectric material, the reduced constitutive equations can be written in terms of shear stress T_5 and strain S_5 and through-thickness electric field E_3 and displacement D_3

$$\begin{Bmatrix} D_3 \\ S_5 \end{Bmatrix} = \begin{bmatrix} \in_{11}^{T} & d_{15} \\ d_{15} & s_{55}^{E} \end{bmatrix} \begin{Bmatrix} E_3 \\ T_5 \end{Bmatrix} \tag{1}$$

where $\in_{11}^{T}$ is the dielectric coefficient for constant stress, d_{15} is the thickness-shear mode piezoelectric coefficient, and s_{55}^{E} is the transverse shear compliance for constant electric field.

Supposing both electric field and displacement to be constant through-thickness and introducing the capacitance of the piezoelectric patch at constant stress, then

$$D_3 = \frac{Q_3}{A},\ E_3 = \frac{V_3}{h},\ C_P^T = \frac{\in_{11}^{T} A}{h} \tag{2}$$

where Q_3 is the charge collected on the electrode area A, V_3 is the difference of electric potential in the upper and lower electrodes, and h is the piezoelectric patch thickness.

Substituting Eq. (2) into Eq. (1) and using the relation between electric current and charge flux such that $I_3 = sQ_3$, where *s* is the Laplace variable, Eq. (1) can be rewritten as

$$\begin{Bmatrix} I_3 \\ S_5 \end{Bmatrix} = \begin{bmatrix} sC_P^T & sAd_{15} \\ \dfrac{d_{15}}{h} & s_{55}^{E} \end{bmatrix} \begin{Bmatrix} V_3 \\ T_5 \end{Bmatrix} \tag{3}$$

Then, introducing Z_{oc}^{T} as the open circuit (OC) electrical impedance for constant stress,

$$Z_{oc}^{T} = \frac{1}{sC_P^T} \tag{4}$$

it is possible to express Eq. (3) in terms of the piezoelectric patch impedance

$$\begin{Bmatrix} I_3 \\ S_5 \end{Bmatrix} = \begin{bmatrix} \dfrac{1}{Z_{oc}^{T}} & sAd_{15} \\ \dfrac{d_{15}}{h} & s_{55}^{E} \end{bmatrix} \begin{Bmatrix} V_3 \\ T_5 \end{Bmatrix} \tag{5}$$

To introduce the shunted damping aspect, let us add a shunt impedance in parallel to the piezoelectric patch, as shown in Fig. 1. It can be noticed that the piezoelectric patch can be represented as an equivalent capacitance.

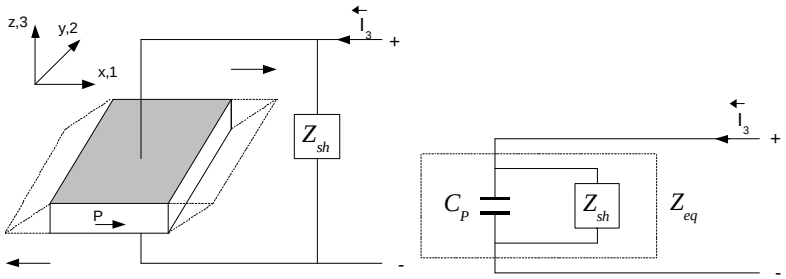

Figure 1. Representation of a piezoelectric capacitance in parallel with a shunt impedance.

These systems can be replaced by an equivalent impedance of similar electric behavior

$$Z_{eq} = \frac{Z_{oc}^{T} Z_{sh}}{Z_{oc}^{T} + Z_{sh}} \tag{6}$$

Then, the first line of Eq. (5) may be solved for V_3, such that

$$V_3 = Z_{eq}\left(I_3 - sAd_{15}T_5\right) \tag{7}$$

which, when replaced in the second line of Eq. (5), yields an expression for the shear strain in terms of shear stress and electric current

$$S_5 = s_{55}^E\left(1 - s\frac{Ad_{15}^2}{s_{55}^E h}Z_{eq}\right)T_5 + \left(\frac{d_{15}}{h}Z_{eq}\right)I_3 \tag{8}$$

Analysis of Eq. (8) allows observing that the coupling of a shunt circuit to the piezoelectric patch yields a modification of the patch compliance. To further investigate this effect, let us define the thickness-shear mode electromechanical coupling coefficient (EMCC) and the equivalent electrical impedance normalized by the open circuit impedance

$$k_{15} = \frac{d_{15}}{\sqrt{s_{55}^E \in_{11}^T}},\ \overline{Z}_{eq} = \frac{Z_{eq}}{Z_{oc}^T} \tag{9}$$

Using Eq. (9) and definitions of C_P^T and Z_{oc}^T, Eqs. (2) and (4), the shear strain is written as

$$S_5 = s_{55}^{sh}T_5 + \left(\frac{d_{15}}{h}Z_{eq}\right)I_3 \tag{10}$$

where s_{55}^{sh} is a modified elastic compliance for the shear piezoelectric patch connected to the shunt circuit

$$s_{55}^{sh} = s_{55}^E\left(1 - k_{15}^2\overline{Z}_{eq}\right) \tag{11}$$

Notice that the shunt modified elastic compliance depends on the short circuit (SC) elastic compliance s_{55}^E, that is for nul electric field, and also on the piezoelectric patch and shunt circuit impedances. Hence, it is possible to derive the equivalent elastic compliance for the standard cases of open (OC) and short circuit (SC) by noting that an open circuit condition may be achieved by letting the shunt circuit impedance tend to infinity, $Z_{sh} \to \infty$, so that

$$\overline{Z}_{eq} = 1 \text{ and } s_{55}^{sh} = s_{55}^D = s_{55}^E\left(1 - k_{15}^2\right) \tag{12}$$

and conversely a short circuit condition is obtained for a nul shunt impedance $Z_{sh} = 0$, so that

$$\overline{Z}_{eq} = 0 \text{ and } s_{55}^{sh} = s_{55}^E \tag{13}$$

Inverting Eq. (10) to obtain stress as function of strain and electric field, leads to

$$T_5 = c_{55}^{sh}S_5 - e_{15}^{sh}E_3 \tag{14}$$

where the new material coefficients are defined as

$$c_{55}^{sh} = \frac{1}{s_{55}^{sh}},\ e_{15}^{sh} = \frac{d_{15}}{s_{55}^{sh}},\ E_3 = \frac{V_3}{h} = \frac{Z_{eq}I_3}{h} \tag{15}$$

For the sake of simplicity, the short circuit, open circuit and shunted shear moduli are defined as $G^{sc} = c_{55}^E$, $G^{oc} = c_{55}^D$, $G^{sh} = c_{55}^{sh}$, respectively. Hence, one may write the shunted shear modulus in terms of short circuit one as

$$G^{sh} = \frac{1}{\left(1 - k_{15}^2\overline{Z}_{eq}\right)}G^{sc} \tag{16}$$

2.2. Case of a Resistive Shunt Circuit

For a resistive shunt circuit, the impedance Z_{sh} resumes to the resistance R considered, such that $Z_{sh} = R$. Therefore, in this case, the normalized equivalent electrical impedance is

$$\bar{Z}_{eq} = \frac{sRC_P^T}{1+sRC_P^T} \tag{17}$$

Considering a harmonic excitation with frequency ω, such that $s = i\omega$, and using Eqs. (16) and (17), the shear modulus for the shunted piezoelectric patch can be rewritten as the following complex modulus

$$G^{sh*} = \left[\frac{1+i\omega RC_P^T}{1+i\omega RC_P^T\left(1-k_{15}^2\right)}\right]G^{sc} \tag{18}$$

Introducing C_p^S as the piezoelectric capacitance at constant strain (nul strain), such that $C_p^S = C_p^T\left(1-k_{15}^2\right)$, and defining ρ as a non-dimensional resistance or frequency,

$$\rho = RC_p^S\omega \tag{19}$$

the shunted complex shear modulus can be written as

$$G^{sh*} = \left[\frac{1}{\left(1-k_{15}^2\right)} - \frac{k_{15}^2\left(1-i\rho\right)}{\left(1-k_{15}^2\right)\left(1+\rho^2\right)}\right]G^{sc} \tag{20}$$

Equation (20) may then be used to derive an equivalent shunted damping loss factor. For that, Eq. (20) is rewritten in the standard complex modulus form

$$G^{sh*} = G_R^{sh}\left(1+i\eta\right) \tag{21}$$

where the real part G_R^{sh} is defined as the storage modulus and the ratio between the imaginary and real parts η is defined as the loss factor. Notice that both are frequency-dependent, since they are written in terms of ρ as

$$G_R^{sh}\left(\rho\right) = \left[\frac{\left(1-k_{15}^2\right)+\rho^2}{\left(1-k_{15}^2\right)\left(1+\rho^2\right)}\right]G^{sc} \text{ and } \eta\left(\rho\right) = \frac{\rho k_{15}^2}{\left(1-k_{15}^2\right)+\rho^2} \tag{22}$$

Notice that analysis of Eq. (22) allows the comparison between damping performance, or loss factor levels, for several shear piezoelectric patches and shunt resistances, since the loss factor depends on the material electromechanical coupling coefficient and on the non-dimensional frequency. In particular, analysis of the loss factor for a thickness-shear mode PZT-5H piezoelectric material $(k_{15} = 0.67)$ connected a resistive shunt circuit in terms of the non-dimensional frequency shows that a 31% loss factor is achievable by properly tuning the shunt circuit resistance or the excitation frequency (Trindade and Maio, 2006). This fact justifies the use of a shunted shear piezoelectric patch for structural vibration damping. Notice that the achievable loss factor for extension piezoelectric is much smaller since its electromechanical coupling coefficient k_{31} is lower.

Due to the frequency-dependent behavior of the shunted shear piezoelectric loss factor, there is an optimal frequency/resistance range of interest in order to obtain a maximum loss factor. From Eq. (22), it is possible indeed to show that the maximum loss factor and the corresponding non-dimensional frequency are

$$\eta_{\max} = \frac{k_{15}^2}{2\sqrt{1-k_{15}^2}} \text{ for } \rho_{op} = \sqrt{1-k_{15}^2} \tag{23}$$

Since $\rho = \omega RC_p^S$, an expression for the shunt circuit resistance that maximizes the loss factor in terms of the excitation frequency can be obtained as

$$R_{op} = \frac{1}{\omega C_p^T\sqrt{1-k_{15}^2}} \tag{24}$$

Hence, Eq. (24) can be used to adjust the shunt circuit resistance so that it leads to a maximum loss factor for a given operating frequency-range.

3. MODELING OF SANDWICH BEAMS WITH SHUNTED SHEAR PIEZOELECTRIC PATCHES

From the previous section, it is clear that a shear piezoelectric patch connected to a properly tuned resistive shunt circuit dissipates a significant amount of energy when excited at a certain frequency-range. Therefore, it is of great interest to integrate such mechanism to a vibrating structure so that its vibratory energy can be dissipated by the shunted piezoelectric patch. According to previous studies (Benjeddou, Trindade and Ohayon, 1999), it is possible to couple bending vibrations of a sandwich beam with the shear strains of a longitudinally-poled piezoelectric patch embedded in the sandwich beam core. This is done here using a sandwich beam finite element model (Benjeddou, Trindade and Ohayon, 1999) in which the individual stiffness matrices for the elastic structure and the piezoelectric patches can be separated, in such way that the equations of motion are written as

$$M\ddot{q}(t)+(K_S+K_P)q(t)=F(t) \tag{25}$$

where M, K_S, K_P are the mass matrix and the elastic structure and piezoelectric patches stiffness matrices, respectively. F is the vector of external applied mechanical forces. The individual stiffness matrices K_S and K_P are obtained in two steps. First, the total stiffness matrix K_T, corresponding to the elastic structure and piezoelectric patches, is obtained using short circuit (for nul electric field) piezoelectric material properties, such that

$$K_T=K_S+\sum_m K_{Pm}^{sc} \tag{26}$$

where $m=1,\ldots,N$ with N being the number of piezoelectric patches. Then, the elastic structure stiffness matrix is obtained by making all elastic, piezoelectric and dielectric constants of the piezoelectric patches to vanish. Consequently, the contribution of each piezoelectric patch to the total stiffness matrix can be evaluated as

$$K_{Pm}^{sc}=K_T-\left(K_S+\sum_{n\neq m}K_{Pn}^{sc}\right) \tag{27}$$

In order to account for the coupling between the piezoelectric patches and the shunt circuits, the short circuit shear modulus is factored out of the piezoelectric stiffness matrices, such that

$$K_{Pm}^{sc}=\overline{K}_{Pm}G_m^{sc} \tag{28}$$

and the equations of motion are written as

$$M\ddot{q}(t)+C\dot{q}(t)+\left(K_S+\sum_m\overline{K}_{Pm}G_m^{sc}\right)q(t)=F(t) \tag{29}$$

where a damping matrix C, corresponding to all other sources of damping, is added *a posteriori*.

Then, for the case of piezoelectric patches connected to resistive shunt circuits subjected to harmonic excitation, the short circuit shear modulii G_m^{sc} can be replaced by their equivalent shunted complex modulii G_m^{sh*}. Consequently, Eq. (29) can be rewritten in the frequency-domain as

$$\left\{-\omega^2M+i\omega C+K_S+\sum_m\overline{K}_{Pm}G_{mR}^{sh}(\omega)[1+i\eta_m(\omega)]\right\}q_0=F_0 \tag{30}$$

where q_0 and F_0 are the amplitudes of the generalized displacements $q(t)$ and applied forces $F(t)$, respectively.

4. SHUNT DAMPING EVALUATION USING MSE METHOD

To evaluate the damping added by the shunted piezoelectric patches to the structure, an iterative version of the Modal Strain Energy (MSE) method, as proposed in (Trindade, Benjeddou and Ohayon, 2000; Johnson and Kienholz, 1982) for structures with viscoelastic elements, is considered. In fact, each shunted piezoelectric patch behaves much like a viscoelastic material, that is, it adds an imaginary part to its stiffness and makes the stiffness dependent on frequency. In the MSE method, the modal damping added to the structure by one of its elements is approximated by the energy fraction contained in the corresponding element multiplied by the element loss factor and divided by the total

strain energy of the structure when it vibrates in one of its eigenmodes. The energy ratio is normally measured as the ratio between modal stiffnesses, such that the damping (loss factor) added by the *m*-th piezoelectric patch is

$$\eta_j^m = \eta_m \frac{\phi_j^T K_{PmR} \phi_j}{\phi_j^T K_T \phi_j} \tag{31}$$

where, in the present case, the stiffness of the *m*-th piezoelectric patch connected to a shunt circuit is $K_{PmR} = \overline{K}_{Pm} G_{mR}^{sh}$.

In the case of a frequency-dependent stiffness, the evaluation of the structure real eigenmodes must be done iteratively from Eq. (30), ignoring the complex terms,

$$\left[-\omega_j^2 M + K_S + \sum_m \overline{K}_{Pm} G_{mR}^{sh}(\omega_j) \right] \phi_j = 0 \tag{32}$$

where ω_j are the structure eigenfrequencies to be evaluated.

Also, each piezoelectric patch stiffness is also dependent on the electric resistance of the shunt circuit connected to it, as shown in section 2. The electric resistance, however, can be tuned to optimize the damping of a selected mode. This is done here by defining the (optimal) resistance of the shunt circuit tuned to damp the *m*-th eigenmode as

$$R_{op}^m = \frac{1}{\omega_m C_p^T \sqrt{1 - k_{15}^2}} \tag{33}$$

To simplify the eigenfrequencies evaluation, an initial guess of the optimal resistances is performed based on the behavior of the storage modulus curves. That is, for the evaluation of the *m*-th optimal resistance, it is supposed that the *k*-th $(k = 1, \ldots, m-1)$ shunted piezoelectric patches are in open-circuit condition; while the *l*-th $(l = m+1, \ldots, N)$ shunted piezoelectric patches are in short-circuit condition. Hence, the stiffness of all shunted piezoelectric patches is properly approximated.

Replacing the expression for the non-dimensional frequency $\rho_m = R_{op}^m C_p^S \omega_j$ in the equations of storage modulus G_{mR}^{sh} and loss factor η_m of each piezoelectric patch, yields

$$G_{mR}^{sh}(\omega_j, R_{op}^m) = \left\{ \frac{\left(1 - k_{15}^2\right) + \left(R_{op}^m C_p^S \omega_j\right)^2}{\left(1 - k_{15}^2\right)\left[1 + \left(R_{op}^m C_p^S \omega_j\right)^2\right]} \right\} G^{sc} \tag{34}$$

$$\eta_m(\omega_j, R_{op}^m) = \frac{\left(R_{op}^m C_p^S \omega_j\right) k_{15}^2}{\left(1 - k_{15}^2\right) + \left(R_{op}^m C_p^S \omega_j\right)^2} \tag{35}$$

An iterative algorithm for the MSE method, shown in Fig. 2, was used in which the evaluation of the *j*-th eigenfrequency is performed accounting for the updating of the *j*-th optimal resistance, whenever the *j*-th eigenmode is being damped by some shunted piezoelectric patch, and of the *j*-th storage modulus.

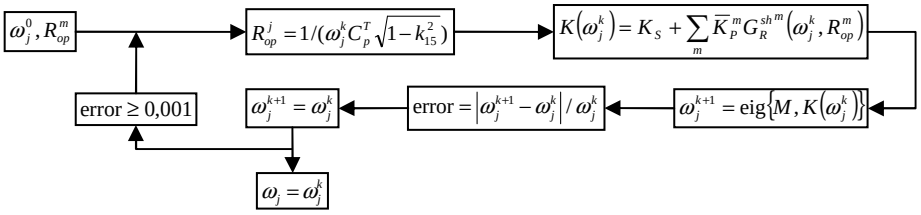

Figure 2. Iterative algorithm for the evaluation of the structure eigenfrequencies accounting for changes in stiffness of shunted piezoelectric patches.

From Eqs. (34) and (35) and recalling that a damping factor relates to a loss factor as $\zeta = \eta/2$, the *j*-th modal damping factor of the structure is written as

$$\zeta_j = \frac{1}{2}\sum_m \frac{\left(R_{ot}^m C_p^S \omega_j\right) k_{15}^2}{\left(1-k_{15}^2\right)+\left(R_{ot}^m C_p^S \omega_j\right)^2} \frac{\phi_j^T \overline{K}_{Pm} G_{mR}^{sh} \phi_j}{\phi_j^T K_T \phi_j} \tag{37}$$

This expression accounts for the contributions of all shunted piezoelectric patches for a given eigenmode. It is expected that the shunted piezoelectric patch which is tuned for a given eigenfrequency should be responsible for the major contribution for the corresponding eigenfrequency. However, as it is illustrated later, other shunted piezoelectric patches could also have a significant contribution.

5. NUMERICAL RESULTS

To illustrate the methodology proposed in the previous sections, it is now applied to a cantilever sandwich beam with three piezoelectric patches embedded in its core layer, as shown in Fig. 3.

The geometrical properties of the structure, shown in Fig. 3, are based on a previous study, which has shown that relatively thick facing layers lead to higher shear strain energy in the piezoelectric patches (Trindade and Maio, 2006). In order to evaluate optimal ranges for position and length of the piezoelectric patches, the following geometric parameters are varied: the distance *d* between the first piezoelectric patch and the clamped end, the spacing *e* between the patches and the length *L* of the patches. The material properties are: Young modulus 210 GPa, Poisson ratio 0.3 and density 7850 kg m^{-3} for the steel; Young modulus 35.3 MPa, shear modulus 12.76 MPa and density 32 kg m^{-3} for the rigid foam; Young modulus 61.1 GPa (SC), shear modulus 23 GPa (SC), density 7500 kg m^{-3}, shear piezoelectric coefficient 17 C m^{-2} and constant stress dielectric coefficient 27.7 nF m^{-1} for the PZT-5H piezoceramic material.

A parametric analysis was performed to evaluate the effects of the distance, spacing and length of the piezoelectric patches on the passive shunted damping. Three values for the piezoelectric patches length were considered: 25 mm, 20 mm and 15 mm. For each of the lengths, the distance from the clamp and the spacing between patches were varied defining a set of geometric configurations. For each configuration, the choice of the eigenmodes to be damped by each piezoelectric patch was performed by, first, tuning each shunted piezoelectric patch to the three selected eigenmodes (3rd, 4th and 5th), one at a time. Then, the damping factors provided for each eigenmode and for each patch are compared and the pair patch-eigenmode leading to the highest damping factor is selected. This procedure is repeated until all piezoelectric patches are assigned to one eigenmode each. This procedure aims to assure patch-eigenmode assignments that maximize the overall damping for each geometric configuration. Then, using the three selected patch-eigenmode tuned pairs, the modal damping factors for the third, fourth and fifth eigenmodes are evaluated.

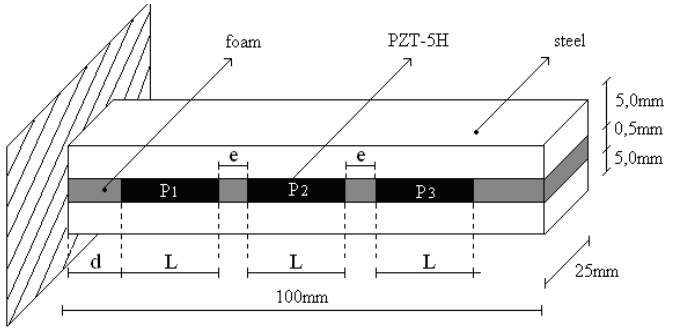

Figure 3. Schematic representation of the cantilever sandwich beam with three piezoelectric patches (not in scale).

Figure 4 shows the average damping factor as a function of patches spacing and distance and for the three patches lengths considered. It is possible to observe that smaller distances yield higher average damping while the optimal spacing depends on the patches length. The comparison between these results has shown that the higher average damping factor is obtained for *L*=20 mm length patches, spaced by *e*=14 mm and with the first patch *d*=3 mm distant from the clamp. However, average damping factors around 1.5% can be observed throughout the ranges *d*=3-7 mm and *e*=11-14 mm. For the optimal configuration, the average damping factor is 1.54%, while the individual modal damping factors for the third, fourth and fifth modes are, respectively, 0.94%, 1.87% and 1.80%. This damping performance was obtained by tuning the piezoelectric patches P1, P2 and P3 to the 5th, 4th and 3rd eigenmodes, respectively.

Table 1 shows the breakdown of the modal damping factors with individual contributions from each piezoelectric patch to each eigenmode. It can be observed that although each patch was tuned to only one eigenmode, all patches contribute to all eigenmodes, including the 2nd eigenmode which was not included in the tuning. As expected, the largest contributions for the fifth and fourth eigenmodes damping were produced by their assigned patches, P1 and P2, respectively. However, the same behavior was not observed for the third eigenmode, for which the smaller contribution comes from its assigned patch P3. This can be explained by the fact that the third eigenmode was the last one to have a patch assigned to it, due to its overall smaller damping, and thus was assigned to the last patch available (P3).

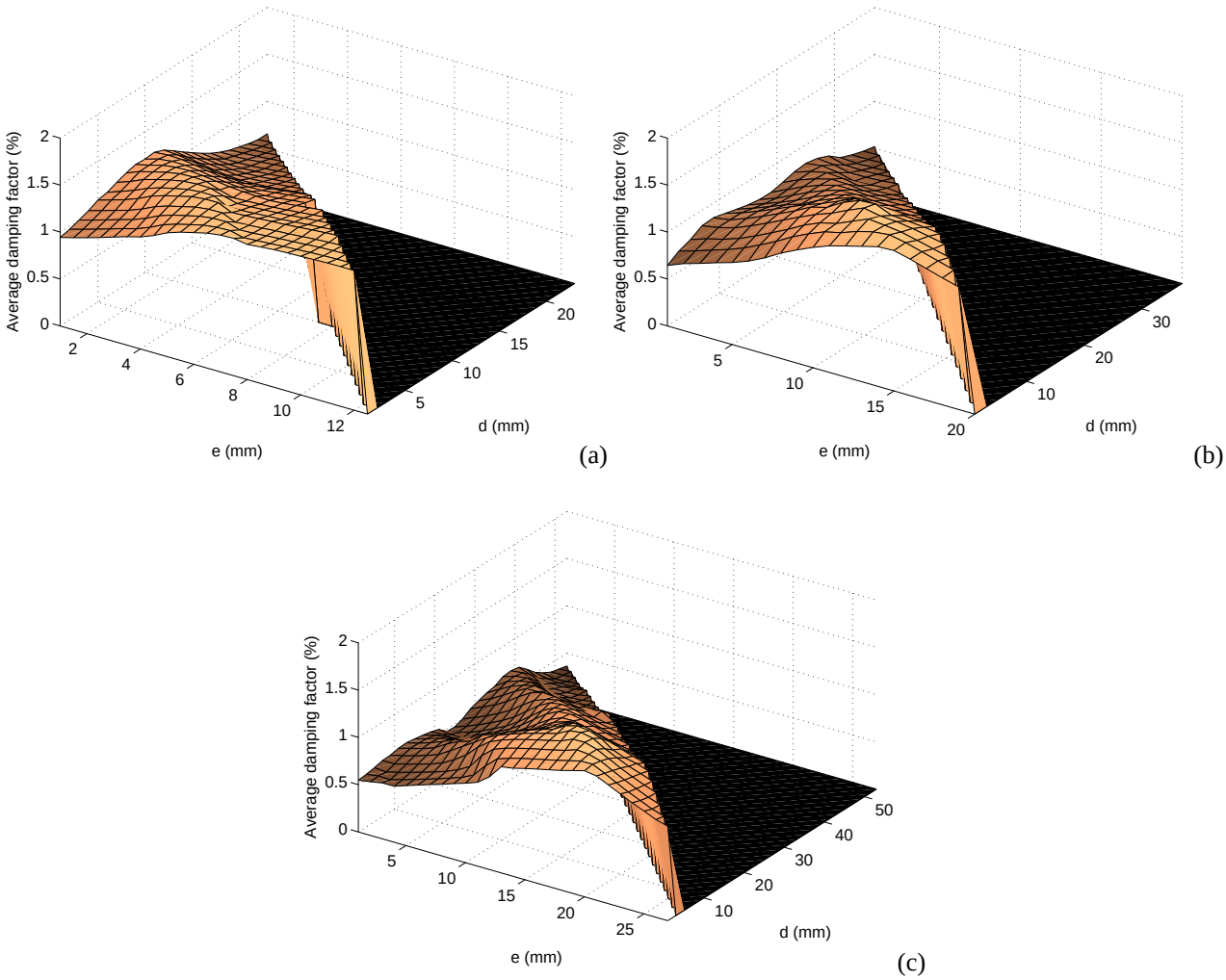

Figure 4. Average damping factors as function of piezoelectric patches spacing *e* and distance *d* for three patches lengths: a) 25 mm, b) 20 mm, b) 15 mm.

Table 1. Damping factors for the second to fifth eigenmodes with individual contributions from each patch and loss factors of each patch at each eigenfrequency.

	Damping factor (%)				Loss factor (%)		
Modes	Patch 1	Patch 2	Patch 3	Total	Patch 1	Patch 2	Patch 3
2	0.13	0.07	0.08	0.28	8.66	13.07	19.90
3	0.31	0.39	0.24	0.94	20.96	27.40	30.86
4	0.65	0.77	0.45	1.87	28.11	30.86	27.40
5	0.93	0.44	0.43	1.80	30.86	28.11	20.96

It is worth noticing that the significant cross-contribution between patches is obtained thanks to the wide frequency range of the shunted patches loss factors, due to the small optimal electric resistance of the corresponding shunt circuits. This fact can also be observed from Fig. 5 and Tab. 1. Table 1 presents also the loss factor of each shunted piezoelectric patch when excited at the second to fifth eigenfrequencies and Fig. 6 shows these loss factors as functions of frequency. It can be observed that, as expected, the maximum loss factor (30.86%) for each patch is obtained at its corresponding tuned eigenfrequency. However, significant loss factor values are maintained at the other eigenfrequencies. In particular, a minimum loss factor of almost 21% is obtained at the 3rd, 4th and 5th eigenfrequencies for all patches. Even at the second eigenfrequency, which was not included in the tuning procedure, loss factors up to 20% are obtained for the third patch.

The frequency response function of the sandwich beam tip velocity, when excited by a transversal force applied at the same point, was evaluated and is shown in Fig. 6 for the following electric boundary conditions: SC – all patches in short-circuit, OC – all patches in open-circuit and OP – all patches optimally shunted. To help analyzing the damping

performance from the frequency response, a zoom around the 2nd to 5th eigenfrequencies is shown in Fig. 7. For comparison purposes, the uncontrolled beam is supposed to have a constant modal damping factor of 0.16%, representing damping sources other than the shunt circuits.

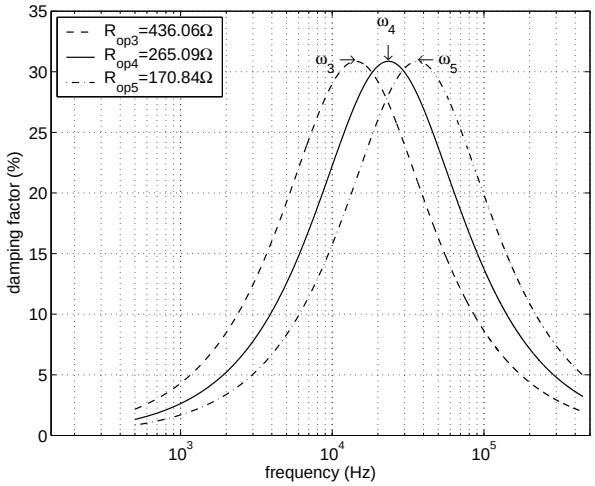

Figure. 5. Loss factor of the three shunted piezoelectric patches tuned to the 3rd, 4th and 5th eigenmodes as a function of frequency.

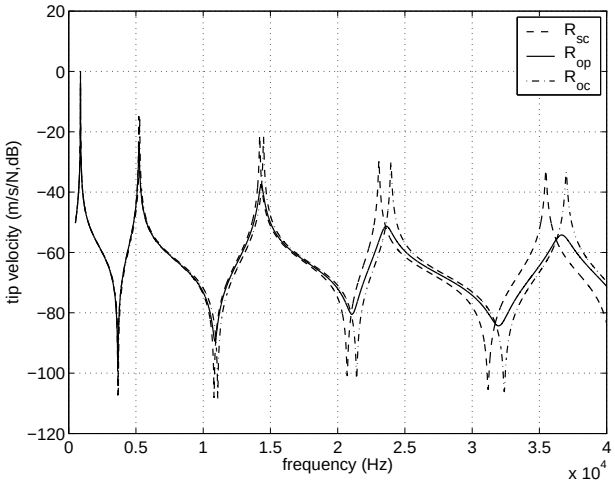

Figure 6. Frequency response function of beam tip velocity with short-circuited (sc), open-circuited (oc) and optimally shunted (op) piezoelectric patches.

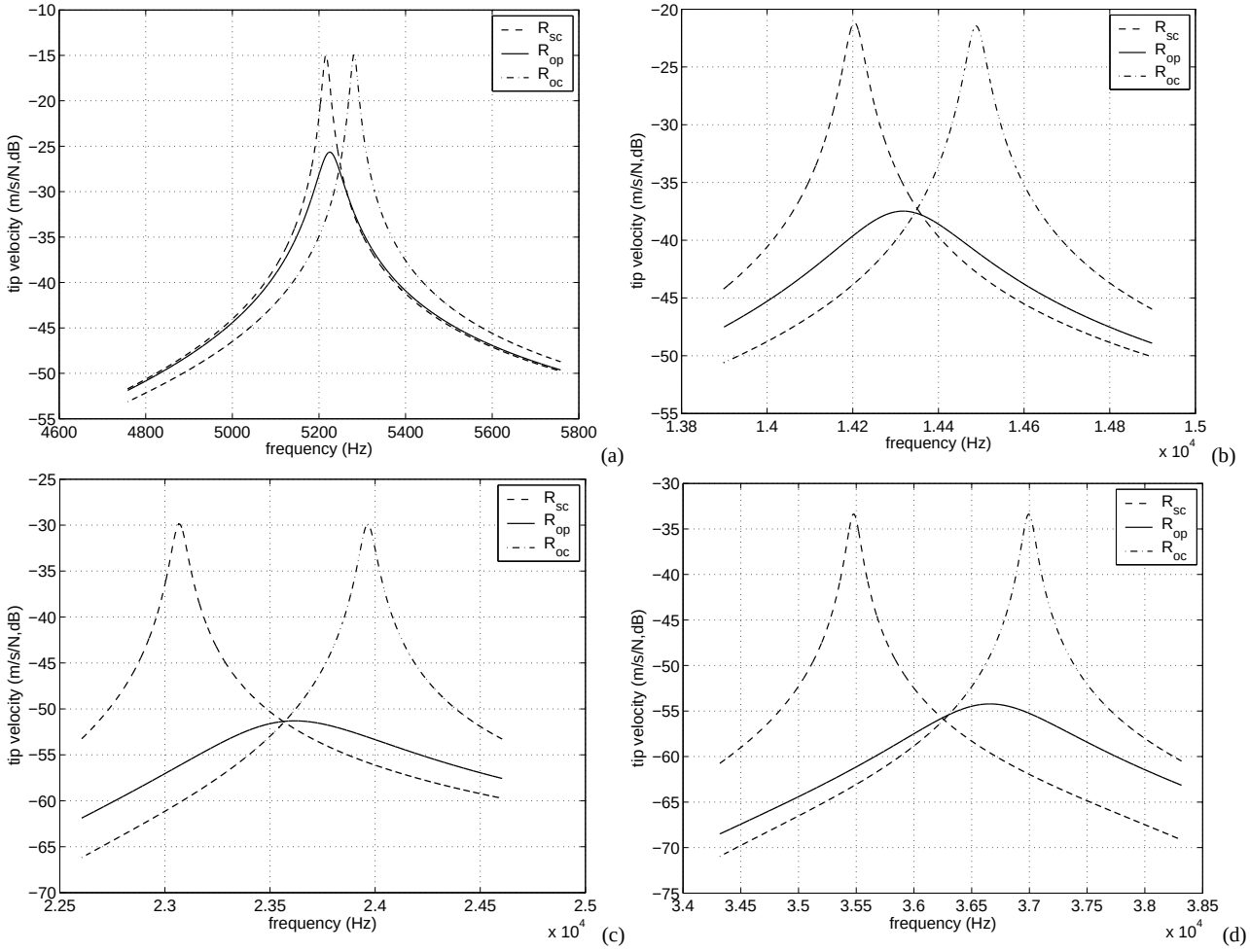

Figure 7. Zoomed frequency response function of the tip velocity of the sandwich beam around eigenfrequencies: (a) 2, (b) 3, (c) 4 and (d) 5.

From Figs. 6 and 7, it is possible to observe that a reduction of approximately 20 dB can be achieved in the amplitude at resonance for the 3rd, 4th and 5th eigenmodes, which were prioritized by the shunted piezoelectric patches. In addition, a reduction of approximately 10 dB is observed for the 2nd eigenmode. These results indicate that not only wider frequency ranges are achievable but also the damping performance of each eigenmode is increased when using a larger number of piezoelectric patches.

6. CONCLUSIONS

This work has presented a performance analysis of the passive vibration control of a sandwich beam using a set of shear piezoelectric patches, embedded in the sandwich beam core and connected to resistive shunt circuits. It was shown that a loss factor of 31% is achievable by shear piezoelectric patches connected to properly tuned resistive shunt circuits. The damping factor added to the structure by each shunted piezoelectric patch was evaluated using an iterative version of the modal strain energy method. Using three shunted piezoelectric patches, tuned to damp the 3rd, 4th and 5th eigenmodes, it was shown that average damping factors up to 1.5% are achievable, yielding a reduction of approximately 20 dB in the vibration amplitude at resonance.

7. ACKNOWLEDGMENTS

This research was supported by the State of São Paulo Research Foundation (FAPESP), through research grants 04/10255-7 and 06/00802-6, which the authors gratefully acknowledge.

8. REFERENCES

Baillargeon, B.P. and Vel, S.S., 2005, “Active vibration suppression of sandwich beams using piezoelectric shear actuators: experiments and numerical simulations”, Journal of Intelligent Materials Systems and Structures, Vol. 16, No. 6, pp.517-530.

Benjeddou, A., 2006, “Shear-mode piezoceramic advanced materials and structures: a state of the art”, to appear in Mechanics of Advanced Materials and Structures.

Benjeddou, A. and Ranger-Vieillard, J.-A., 2004, “Passive vibration damping using shunted shear-mode piezoceramics”, In Topping, B.H.V. and Mota Soares, C.A., eds., Proceedings of the Seventh International Conference on Computational Structures Technology, Civil-Comp Press, Stirling, Scotland, p.#4.

Benjeddou, A., Trindade, M.A., and Ohayon, R., 1999, “New shear actuated smart structure beam finite element”, AIAA Journal, Vol. 37, No. 3, pp.378-383.

Forward, R.L., 1979, “Electronic damping of vibrations in optical structures”, Applied Optics, Vol. 18, No. 5, pp.690-697.

Hagood, N.W. and von Flotow, A., 1991, “Damping of structural vibrations with piezoelectric materials and passive electrical networks”, Journal of Sound and Vibration, Vol. 146, No. 2, pp.243-268.

Johnson, C.D. and Kienholz, D.A., 1982, “Finite element prediction of damping in structures with constrained viscoelastic layers”, AIAA Journal, 20(9):1284-1290.

Raja, S., Prathap, G., and Sinha, P.K., 2002, “Active vibration control of composite sandwich beams with piezoelectric extension-bending and shear actuators”, Smart Materials and Structures, Vol. 11, No. 1, pp.63-71.

Sunar, M. and Rao, S.S., 1999, “Recent advances in sensing and control of flexible structures via piezoelectric materials technology”, Applied Mechanics Review, Vol. 52, No. 1, pp. 1-16.

Sun, C.T. and Zhang, X.D., 1995, “Use of thickness-shear mode in adaptive sandwich structures”, Smart Materials and Structures, Vol. 4, No. 3, pp.202-206.

Trindade, M.A., Benjeddou, A., and Ohayon, R., 1999, “Parametric analysis of the vibration control of sandwich beams through shear-based piezoelectric actuation”, Journal of Intelligent Materials Systems and Structures, Vol. 10, No. 5, pp.377-385.

Trindade, M.A., Benjeddou, A., and Ohayon, R., 2000, “Modeling of frequency-dependent viscoelastic materials for active-passive vibration damping”, Journal of Vibration and Acoustics, 122:169-174.

Trindade, M.A. and Maio, C.E.B., 2006, “Passive vibration control of sandwich beams using shunted shear piezoelectric actuators”, in IV Congresso Nacional de Engenharia Mecânica, Recife, ABCM.

9. RESPONSIBILITY NOTICE

The authors are the only responsible for the printed material included in this paper.